Nonequilibrium relaxation of the two-dimensional Ising model: Series-expansion and Monte Carlo studies

Jian-Sheng Wang[†] and Chee Kwan Gan[†‡]
[†]*Department of Computational Science, National University of Singapore, Singapore 119260, Republic of Singapore.*
[‡]*Cavendish Laboratory, University of Cambridge, Madingley Road, Cambridge CB3 0HE, United Kingdom.*
(17 December 1997)

We study the critical relaxation of the two-dimensional Ising model from a fully ordered configuration by series expansion in time t and by Monte Carlo simulation. Both the magnetization (m) and energy series are obtained up to 12-th order. An accurate estimate from series analysis for the dynamical critical exponent z is difficult but compatible with 2.2. We also use Monte Carlo simulation to determine an effective exponent, $z_{\rm eff}(t) = -\frac{1}{8} d \ln t / d \ln m$, directly from a ratio of three-spin correlation to m. Extrapolation to $t \to \infty$ leads to an estimate $z = 2.169 \pm 0.003$.

PACS number(s): 05.50.+q, 05.70.Jk, 02.70.Lq

I. INTRODUCTION

The pure relaxational dynamics of the kinetic Ising model with no conserved fields, which is designated as model A in the Hohenberg-Halperin review [1], has been studied extensively by various approaches. Unlike some of the other models in which the dynamical critical exponent z can be related to the static exponents, it seems that z of model A is independent of the static exponents (however, see Ref. [2]). In the past twenty years, the numerical estimates for the dynamical critical exponent z scattered a lot, but recent studies seem to indicate a convergence of estimated values. Our studies contribute further to this trend.

We review briefly some of the previous work on the computation of the dynamical critical exponents, concentrating mostly on the two-dimensional Ising model. The conventional theory predicts $z = 2 - \eta$ [3], where η is the critical exponent in the two-point correlation function, $G(r) \propto r^{-d+2-\eta}$. For the two-dimensional Ising model, this gives $z = 1.75$. It is known that this is only a lower bound [4]. It is very interesting to note that series expansions [5–10] gave one of the earliest quantitative estimates of z. Dammann and Reger [10] have the longest high-temperature series (20 terms) for the relaxation times so far, obtaining $z = 2.183 \pm 0.005$. However, re-analysis of the series by Adler [11] gives $z = 2.165 \pm 0.015$. There are two types of field-theoretic renormalization group analysis: the ϵ-expansion near dimension $d = 4$ [12,13] and an interface model near $d = 1$ [14]. It is not clear how reliable when it is interpolated to $d = 2$. Real-space renormalization group of various schemes has been proposed in the early eighties [15–18], but it appears that there are controversies as whether some of the schemes are well-defined. The results are not of high accuracy compared to other methods. Dynamic Monte Carlo renormalization group [19–22] is a generalization of the equilibrium Monte Carlo renormalization group method [23]. The latest work [22] gives $z = 2.13 \pm 0.01$ in two dimensions. Equilibrium Monte Carlo method is one of the standard methods to estimate z [24–28]. However, long simulations ($t \gg L^z$) are needed for sufficient statistical accuracy of the time-displaced correlation functions. The analysis is quite difficult due to unknown nature of the correlation functions. Nonequilibrium relaxation [29–34], starting from a completely ordered state at T_c, has nice features. The analysis of data is more or less straightforward. The lattice can be made very large, so that finite-size effect can be ignored (for $t \ll L^z$). The catch here is that correction to scaling due to finite t is large. Recently, the idea of damage spreading [35–39] has also been employed. Methods based on statistical errors in equilibrium Monte Carlo simulation [40], finite-size scaling of nonequilibrium relaxation [41,42], and finite-size scaling of the eigenvalues of the stochastic matrix [43,44] are used to compute the exponent. A recent calculation with a variance-reducing Monte Carlo algorithm for the leading eigenvalues gives prediction [44] $z = 2.1665 \pm 0.0012$. This appears to be the most precise value reported in the literature.

The high-temperature series expansions for the relaxation times are often used in the study of Ising dynamics. In this paper, we present a new series which directly corresponds to the magnetization (or energy) relaxation at the critical temperature. Our series expansion method appears to be the only work which uses time t as an expansion parameter. The generation of these series is discussed in Sections II and III. Dynamical scaling mentioned in Section IV forms the basis of the analysis, and the results are analyzed in Section V. We feel that the series are still too short to capture the dynamics at the scaling regime. We also report results of an extensive Monte Carlo simulation for the magnetization relaxation. We find that it is advantageous to compute an effective dynamical critical exponent directly with the help of the governing master equation (or the rate equation). The

simulation and analysis of Monte Carlo data are presented in Section VI. We summarize and conclude in Section VII.

II. SERIES EXPANSION METHOD

In this section, we introduce the relevant notations, and outline our method of series expansion in time variable t. The formulation of single-spin dynamics has already been worked out by Glauber [45], and by Yahata and Suzuki [5] long time ago. To our knowledge, all the previous series studies for Ising dynamics [5–10] are based on high-temperature expansions of some correlation times. As we will see, expansion in t is simple in structure, and it offers at least a useful alternative for the study of Ising relaxation dynamics.

We consider the standard Ising model on a square lattice [46] with the energy of a configuration σ given by

$$E(\sigma) = -J \sum_{\langle i,j \rangle} \sigma_i \sigma_j, \tag{1}$$

where the spin variables σ_i take ± 1, J is the coupling constant, and the summation runs over all nearest neighbor pairs. The thermal equilibrium value of an observable $f(\sigma)$ at temperature T is computed according to the Boltzmann distribution,

$$\langle f \rangle = \frac{\sum_\sigma f(\sigma) \exp\bigl(-E(\sigma)/k_B T\bigr)}{\sum_\sigma \exp\bigl(-E(\sigma)/k_B T\bigr)} = \sum_\sigma f(\sigma) P_{\rm eq}(\sigma). \tag{2}$$

The equilibrium statistical-mechanical model defined above has no intrinsic dynamics. A local stochastic dynamics can be given and realized in Monte Carlo simulations [47]. The dynamics is far from unique; in particular, cluster dynamics [48] differs vastly from the local ones.

A sequence of Monte Carlo updates can be viewed as a discrete Markov process. The evolution of the probability distribution is given by

$$P(\sigma, k+1) = \sum_{\sigma'} P(\sigma', k) W(\sigma'|\sigma), \tag{3}$$

where W is a transition matrix satisfying the stationary condition with respect to the equilibrium distribution, i.e., $P_{\rm eq} = P_{\rm eq} W$. A continuous time description is more convenient for analytic treatment. This can be obtained by fixing $t = k/N$, and letting $\delta t = 1/N \to 0$, where $N = L^2$ is the number of spins in the system. The resulting differential equation is given by

$$\frac{\partial P(\sigma, t)}{\partial t} = \Gamma P(\sigma, t), \tag{4}$$

where Γ is a linear operator acting on the vector $P(\sigma, t)$, which can be viewed as a vector of dimension 2^N, indexed by σ. If we use the single-spin-flip Glauber dynamics [45], we can write

$$\Gamma = -\sum_{j=1}^{N} w_j(\sigma_j) + \sum_{j=1}^{N} w_j(-\sigma_j) F_j, \tag{5}$$

where

$$w_j(\sigma_j) = \frac{1}{2}\Bigl[1 - \sigma_j \tanh\Bigl(K \sum_{\text{nn of j}} \sigma_k\Bigr)\Bigr],\ K = \frac{J}{k_B T}, \tag{6}$$

and F_j is a flip operator such that

$$F_j P(\ldots, \sigma_j, \ldots) = P(\ldots, -\sigma_j, \ldots). \tag{7}$$

The flip rate $w_j(\sigma_j)$ for site j depends on the spin value at the site j as well as the values of its nearest neighbor spins σ_k.

The full probability distribution clearly contains all the dynamic properties of the system. Unfortunately its high dimensionality is difficult to handle. It can be shown from the master equation, Eq. (4), that any function of the state σ (without explicit t dependence) obeys the equation

$$\frac{d\langle f \rangle_t}{dt} = -\langle \mathcal{L} f \rangle_t, \tag{8}$$

where

$$\mathcal{L} = \sum_{j=1}^{N} w_j(\sigma_j)(1 - F_j), \tag{9}$$

and the average of f at time t is defined by

$$\langle f \rangle_t = \sum_\sigma f(\sigma) P(\sigma, t). \tag{10}$$

Note that the time dependence of $\langle f \rangle$ is only due to $P(\sigma, t)$. For the series expansion of this work, it is sufficient to look at a special class of functions of the form $\sigma^A = \prod_{j \in A} \sigma_j$, where A is a set of sites. In such a case we have

$$\frac{d\langle \sigma^A \rangle_t}{dt} = -2 \sum_{j \in A} \bigl\langle w_j(\sigma_j) \sigma^A \bigr\rangle_t. \tag{11}$$

With this set of equations, we can compute the n-th derivative of the average magnetization $\langle \sigma_0 \rangle_t$. A formal solution to Eq. (8) is

$$\langle \sigma^A \rangle_t = \bigl\langle e^{-\mathcal{L}t} \sigma^A \bigr\rangle_0 = \sum_{n=0}^{\infty} \left\langle \frac{(-\mathcal{L}t)^n}{n!} \sigma^A \right\rangle_0. \tag{12}$$

This equation or equivalently the rate equation, Eq. (11), forms the basis of our series expansion in time t.

A few words on high-temperature expansions are in order here. They are typically done by integrating out

the time dependence—the nonlinear relaxation time can be defined as

$$\tau_{\rm nl}^A = \int_0^\infty \langle \sigma^A \rangle_t dt = \left\langle \int_0^\infty dt\, e^{-\mathcal{L}t} \sigma^A \right\rangle_0 = \langle \mathcal{L}^{-1} \sigma^A \rangle_0. \tag{13}$$

The equilibrium correlation time (linear relaxation time) can be expressed as

$$\tau = \int_0^\infty \frac{\langle m(0)m(t)\rangle_{\rm eq}}{\langle m(0)^2\rangle_{\rm eq}} dt = \sum_j \int_0^\infty \langle \sigma_0 e^{-\mathcal{L}t} \sigma_j \rangle_{\rm eq}/\chi$$
$$= \frac{1}{\chi} \sum_j \langle \sigma_0 \mathcal{L}^{-1} \sigma_j \rangle_{\rm eq}. \tag{14}$$

where $\chi = N\langle m^2 \rangle_{\rm eq}$ is the reduced static susceptibility. The average is with respect to the equilibrium distribution, $P_{\rm eq}(\sigma)$. A suitable expansion in small parameter J/k_BT can be made by writing $\mathcal{L} = \mathcal{L}_0 + \Delta\mathcal{L}$.

It is clear that we can also perform the Kawasaki dynamics with a corresponding rate. Of course, since the magnetization is conserved, only energy and higher order correlations can relax.

A very convenient form for the Glauber transition rate, Eq. (6), on a two-dimensional square lattice is

$$w_0(\sigma_0) = \frac{1}{2}\Big[1 + x\sigma_0(\sigma_1+\sigma_2+\sigma_3+\sigma_4) + y\sigma_0(\sigma_1\sigma_2\sigma_3+\sigma_2\sigma_3\sigma_4+\sigma_3\sigma_4\sigma_1+\sigma_4\sigma_1\sigma_2)\Big], \tag{15}$$

$$x = -\frac{1}{4}\tanh 2K - \frac{1}{8}\tanh 4K, \tag{16}$$

$$y = +\frac{1}{4}\tanh 2K - \frac{1}{8}\tanh 4K, \tag{17}$$

where the site 0 is the center site, and sites 1, 2, 3, and 4 are the nearest neighbors of the center site. At the critical temperature, $\tanh K_c = \sqrt{2} - 1$, we have $x = -5\sqrt{2}/24$ and $y = \sqrt{2}/24$.

III. COMPUTER IMPLEMENTATION AND RESULTS

A series expansion in t amounts to finding the derivatives evaluated at $t = 0$:

$$\langle \sigma^A \rangle_t = \sum_{n=0}^\infty \frac{t^n}{n!} \frac{d^n \langle \sigma^A \rangle}{dt^n}\Big|_{t=0}. \tag{18}$$

The derivatives are computed using Eq. (11) recursively. A general function is coded in C programming language to find the right-hand side of Eq. (11) when the configuration σ^A, or the set A, is given. The set A is represented as a list of coordinates constructed in an ordered manner. By specializing the flip rate as given by Eq. (15), and considering each site in A in turn, the configurations on the right-hand side of the rate equation are generated in three ways: (1) the same configuration as A, which contributes a factor (coefficient of a term) of -1; (2) a set of configurations generated by introducing a pair of nearest neighbor sites in four possible directions, with one of the sites being the site in A under consideration, and making use of the fact $\sigma_i^2 = 1$. We notice that the site in A under consideration always gets annihilated. Each resulting configuration contributes a factor of $-x$; and (3) same as in (2) but two more sites which are also the nearest neighbors of the site in A under consideration are introduced. This two extra sites form a line perpendicular to the line joined by the first pair of neighbor sites in (2). Each of this configuration has a factor of $-y$. It is instructive to write down the first rate equation, taking into account of the lattice symmetry (e.g. $\langle \sigma_i \rangle = \langle \sigma_0 \rangle$, for all i):

$$\frac{d\langle \sigma_0 \rangle}{dt} = -(1+4x)\langle \sigma_0 \rangle - 4y\langle \sigma_1\sigma_2\sigma_3 \rangle. \tag{19}$$

The core of the computer implementation for series expansion [49] is a symbolic representation of the rate equations. Each rate equation is represented by a node together with a list of pointers to other nodes. Each node represents a function $\langle \sigma^A \rangle$, and is characterized by the set of spins A. The node contains pointers to the derivatives of this node obtained so far, and pointers to the "children" of this node and their associated coefficients, which form a symbolic representation of the rate equations. The derivatives are represented as polynomials in y. Since each node is linked to other nodes, the computation of the n-th derivative can be thought of as expanding a tree (with arbitrary number of branches) of depth n.

The traversal or expansion of the tree can be done in a depth-first fashion or a breadth-first fashion. Each has a different computational complexity. A simple depth-first traversal requires only a small amount of memory of order n. However, the time complexity is at least exponential, b^n, with a large base b. A breadth-first algorithm consumes memory exponentially, even after the number of the rate equations has been reduced by taking the symmetry of the problem into account. The idea of dynamic programming can be incorporated in the breadth-first expansion where the intermediate results are stored and referred. To achieve the best performance, a hybrid of strategies is used to reduce the computational complexity:

- Each configuration (pattern) is transformed into its canonical representation, since all configurations related by lattice symmetry are considered as the same configuration.
- We use breadth-first expansion to avoid repeated computations involving the same configuration. If

a configuration has already appeared in earlier expansion, a pointer reference is made to the old configuration. Each configuration is stored in memory only once. However, storing of all the distinct configurations leads to a very fast growth in memory consumption.

- The last few generations in the tree expansion use a simple depth-first traversal to curb the problem of memory explosion.

- Parallel computation proves to be useful. The longest series is obtained by a cluster of 16 Pentium Pro PCs with high speed network connection (known as Beowulf).

The program is controlled by two parameters D and C. D is the depth of breadth-first expansion of the tree. When depth D is reached, we no longer want to continue the normal expansion in order to conserve memory. Instead, we consider each leave node afresh as the root of a new tree. The derivatives up to $(n-D)$th order are computed for this leave node. The expansion of the leave nodes are done in serial, so that the memory resource can be reused. The parameter C controls the number of last C generations which should be computed with a simple depth-first expansion algorithm. It is a simple recursive counting algorithm, which uses very little memory, and can run fast if the depth C is not very large. In this algorithm the lattice symmetry is not treated. The best choice of parameters is $D = 6$ and $C = 2$ on a DEC AlphaStation 250/266. The computer time and memory usage are presented in Table I. As we can see from the table, each new order requires more than a factor of ten CPU time and about the same factor for memory if memory is not reused. This is the case until the order $D+C+1$, where no fresh leave-node expansion is made. There is a big jump (a factor of 60) in CPU time from 9-th order to 10-th order, but with a much smaller increase in memory usage. This is due to the change of expansion strategy. Finally the longest 12-th order series is obtained by parallel computation on a 16-node Pentium Pro 200 MHz cluster in 12 days. The number of distinct nodes generated to order n is roughly $\frac{1}{100}11^n$. To 12-th order, we have examined about 10^{10} distinct nodes. The series data are listed in Table II.

IV. DYNAMICAL SCALING

The traditional method of determining the dynamical critical exponent z is to consider the time-displaced equilibrium correlation functions. However, one can alternatively look at the relaxation towards thermal equilibration. The basic assumption is the algebraic decay of the magnetization at T_c,

$$\langle \sigma_0 \rangle = m \approx c\, t^{-\beta/\nu z}, \qquad t \to \infty. \tag{20}$$

This scaling law can be obtained intuitively as follows. Since the relaxation time and the correlation length are related through $\tau \propto \xi^z$ by definition, after time t, the equilibrated region is of size $t^{1/z}$. Each of such region is independent of the others, so the system behaves as a finite system of linear length $\xi \propto t^{1/z}$. According to finite-size scaling [50], the magnetization is of order $\xi^{-\beta/\nu}$ on a finite system of length ξ. Each region should have the same sign for the magnetization since we started the system with all spins pointing in the same direction. The total magnetization is equal to that of a correlated region, giving $m \propto t^{-\beta/\nu z}$.

The same relation can be derived from a more general scaling assumption [51],

$$m(t,\epsilon) \approx \epsilon^\beta \phi(t\epsilon^{\nu z}), \qquad \epsilon = \frac{T - T_c}{T_c}. \tag{21}$$

By requiring that $m(t,\epsilon)$ is still finite as the scaling argument $t\epsilon^{\nu z} \to 0$ and $\epsilon \to 0$ with fixed t, we get Eq. (20).

Equation (20) is only true asymptotically for large t. It seems that there is no theory concerning leading correction to the scaling. As a working hypothesis, we assume that

$$m \approx c\, t^{-\beta/\nu z}(1 + b\, t^{-\Delta}). \tag{22}$$

The Monte Carlo simulation results as well as current series analysis seem to support this with Δ near 1. Other possibility might be $z = 2$ with logarithmic correction [52].

V. ANALYSIS OF SERIES

A general method for extending the range of convergence of a series is the Padé analysis [53,54] where a series is approximated by a ratio of two polynomials. We first look at the poles and zeros of the Padé approximants in variable $s = t/(t+1)$ for m. Since t varies in the range of $[0,\infty)$, it is easier to look at s, which maps the interval $[0,\infty)$ to $[0,1)$. There are clusters of zeros and poles in the s-interval $(1,2)$ which corresponds to negative t. But interval $[0,1)$ is clear of singularities, which gives us hope for analytic continuation to the whole interval $[0,1)$. If we assume the asymptotic behavior $m \propto t^{-a}$, then $d\ln m/dt = -a/t \approx -a(1-s)$ for large t or $s \to 1$. This means that the Padé approximant should give a zero around $s = 1$. We do observe zeros near 1. But it is typically a pair of zeros off the real axis together with a pole at the real axis near 1, or sometimes, only a pair of real zeros. These complications make a quantitative analysis difficult.

Since we know the exact singular point (corresponding to $t = \infty$), we use the biased estimates by considering the function

$$F(t) = \frac{d\ln m}{d\ln t} \approx -\frac{\beta}{\nu z}. \tag{23}$$

An effective exponent $z_{\rm eff}(t)$ is defined by $z_{\rm eff}(t) = -\beta/(\nu F(t)) = -1/(8F(t))$.

Again we prefer to use the variable s to bring the infinity to a finite value 1. Due to an invariance theorem [53], the diagonal Padé approximants in s and t are equal exactly. For off-diagonal Padé approximants, s is more useful since the approximants do not diverge to infinity.

We use methods similar to that of Dickman *et al.* [55] and Adler [11]. The general idea is to transform the function $m(t)$ into other functions which one hopes to be better behaved than the original function. In particular, we require that as $t \to \infty$, the function approaches a constant related to the exponent z. The first transformation is the Eq. (23). A second family of transformations is

$$G_p(t) = \frac{d \ln \int_0^t m(t')^p dt'}{d \ln t} \approx 1 - \frac{p}{8z}, \tag{24}$$

where p is a real positive number. One can show that the two functions are related by

$$F(t) = \frac{1}{p}\left(G_p(t) - 1 + \frac{d \ln G_p(t)}{d \ln t} \right). \tag{25}$$

The last transform is

$$H(t) = F(t) + \frac{1}{\Delta} t \frac{dF}{dt}, \tag{26}$$

where Δ is an adjustable parameter, and F can also be replaced by G_p. If the leading correction to the constant part is of the form $t^{-\Delta}$, the transformation will eliminate this correction term.

The transformation of the independent variable t to other variable is important to improve the convergence of the Padé approximants. We found that it is useful to consider a generalization of the Euler transform,

$$u = 1 - \frac{1}{(1+t)^{\Delta}}. \tag{27}$$

The parameter Δ is adjusted in such a way to get best convergence among the approximants. Since for $t \to \infty$ or $u \to 1$, a Padé approximant near $u = 1$ is an analytic function in u, which implies that the leading correlation is of the form $t^{-\Delta}$. Note that $\Delta = 1$ corresponds to the Euler transformation ($u = s$ when $\Delta = 1$).

One of the fundamental difficulties of the transformation method is that one does not know a priori that a certain transformation is better than others. Worst still, we can easily get misleading apparent convergence among different approximants. Thus, we need to be very careful in interpreting our data. Specifically, we found that Eq. (23) gives less satisfactory result than that of Eq. (24), where the independent variable t is transformed into u according to Eq. (27). Figure 1 is a plot of all the Padé approximants of order $[N, D]$, with $N \geq 4$, $D \geq 4$, and $N + D \leq 12$, as a function of the parameter Δ, for $G_1(t = \infty)$. Good convergence is obtained at $\Delta = 1.217$ with $z \approx 2.170$. The estimates z vary only slightly with p, at about 0.005 as p varies from 0.5 to 2. Using $F(t)$ of Eq. (23), the optimal value is $\Delta = 1.4$ with $z \approx 2.26$. Using the function H does not seem to improve the convergence. Even though the value 2.170 seems to be a very good result, we are unsure of its significance since there are large deviations of the Padé approximation to the function $F(t)$ for $1/t < 0.2$ from the Monte Carlo result of Fig. 2.

An objective error estimate is difficult to give. Estimates from the standard deviation of the approximants tend to give a very small error but incompatible among different methods of analysis. Different Padé approximants are definitely not independent; we found that $[N, D]$ Padé is almost equal to $[D, N]$ Padé to a high precision. A conservative error we quote from the series analysis is 0.1.

Analysis of the energy series is carried out similarly with m replaced by $\langle \sigma_0 \sigma_1 \rangle - \sqrt{2}/2$, where the constant $\sqrt{2}/2$ is the equilibrium value. The large t asymptotic behavior is $t^{-1/z}$ [56]. Both F and G functions give comparable results, better convergence is obtained for $\Delta > 1$. The value for z is about 2.2, but good crossing of the approximants are not observed. We feel better analysis method or longer series is needed.

VI. MONTE CARLO SIMULATION

Our motivation for a Monte Carlo calculation was to check the series result. It turns out that the data are sufficiently accurate to be discussed in their own right. Such an improved accuracy is achieved by using Eq. (19), which permits a direct evaluation of the effective exponent $z_{\rm eff}(t)$.

We compute the magnetization $m = \langle \sigma_0 \rangle$, energy per bond $\langle \sigma_0 \sigma_1 \rangle$, and the three-spin correlation $m_3 = \langle \sigma_1 \sigma_2 \sigma_3 \rangle$ where the three spins are the nearest neighbors of a center site having one of the neighbor missing in the product. With these quantities, the logarithmic derivative, Eq. (23), can be computed exactly without resorting to finite differences. From Eq. (19) we can write (at $T = T_c$)

$$F(t) = \frac{d \ln m}{d \ln t} = -t\left(1 + \frac{\sqrt{2}}{6}\left(\frac{m_3}{m} - 5\right)\right) = -\frac{1}{8 z_{\rm eff}(t)}. \tag{28}$$

The above equation also defines the effective exponent $z_{\rm eff}(t)$ which should approach the true exponent z as $t \to \infty$.

The estimates for the effective exponent based on the ratio of one spin to three-spin correlation, Eq. (28), have smaller statistical errors in comparison to a finite difference scheme based on $m(t)$ and $m(t+1)$. Error propagation analysis shows that the latter has an error 5 times larger. Both methods suffer from the same problem that

error $\delta z \propto t$. Thus, working with very large t does not necessarily lead to any advantage.

In order to use Eq. (28), we need exactly the same flip rate as in the analytic calculations, namely the Glauber rate, Eq. (6). The continuous time dynamics corresponds to a random selection of a site in each step. Sequential or checker-board updating cannot directly be compared with the analytic results. However, it is believed that the dynamical critical exponent z does not depend on the details of the dynamics.

We note that a Monte Carlo simulation is precisely described by a discrete Markov process while the series expansion is based on the continuous master equation. However, the approach to the continuous limit should be very fast since it is controlled by the system size—the discreteness in time is $1/L^2$. We have used a system of $10^4 \times 10^4$, which is sufficiently large. Apart from the above consideration, we also checked finite-size effect. Clearly, as $t > L^z$, finite-size effect begins to show up. We start the system with all spins up, $m(0) = 1$, and follow the system to $t = 99$. For $t < 100$, we did not find any systematic finite-size effect for $L \geq 10^3$. So the finite-size effect at $L = 10^4$ and $t < 100$ can be safely ignored.

Figure 2 shows the Monte Carlo result for the effective exponent as a function of $1/t$. The quantities m, m_3, and $\langle \sigma_0 \sigma_1 \rangle$ are averaged over 1868 runs, each with a system of 10^8 spins. The total amount of spin updating is comparable to the longest runs reported in the literature. Based on a least-squares fit from $t = 30$ to 99, we obtain

$$z = 2.169 \pm 0.003. \tag{29}$$

The error is obtained from the standard deviation of few groups of independent runs. An error estimate based on the residues in the linear least-squares fit is only half of the above value, which is understandable since the points in Fig. 2 are not statistically independent.

In Fig. 2, we also plot a series result for the $F(t)$, obtained from the [6,6] Padé of $G_1(u)$ and Eq. (25). Substantial deviations are observed for $1/t < 0.2$, even though in the $1/t \to 0$ limit, both results are almost the same. This casts some doubts on the reliability of the series analysis. We note that the $t \to \infty$ limit of the function $F(t)$ is invariant against any transformation in t which maps $t = \infty$ to ∞. Thus, the discrepancy might be eliminated by a suitable transformation in the Padé analysis.

VII. CONCLUSION

We have computed series for the relaxation of magnetization and energy at the critical point. The same method can be used to obtain series at other temperatures or for other correlation functions. The analyses of the series are non-trivial. We may need much more terms before we can obtain result with accuracy comparable to the high-temperature series. We have also studied the relaxation process with Monte Carlo simulation. The ratio of three-spin to magnetization is used to give a numerical estimate of the logarithmic derivatives directly. This method gives a more accurate estimate for the dynamical critical exponent.

ACKNOWLEDGMENT

This work was supported in part by an Academic Research Grant No. RP950601.

[1] P. C. Hohenberg and B. I. Halperin, Rev. Mod. Phys. **49**, 435 (1977).
[2] Z. Alexandrowicz, Physica A **167**, 322 (1990).
[3] L. van Hove, Phys. Rev. **93**, 1374 (1954).
[4] R. Abe and A. Hatano, Prog. Theor. Phys. **41**, 941 (1969).
[5] H. Yahata and M. Suzuki, J. Phys. Soc. Jpn. **27**, 1421 (1969).
[6] H. Yahata, J. Phys. Soc. Jpn. **30**, 657 (1971).
[7] Z. Rácz and M. F. Collins, Phys. Rev. B **13**, 3074 (1976).
[8] J. Rogiers and J. O. Indekeu, Phys. Rev. B **41**, 6998 (1990).
[9] J. Wang, Phys. Rev. B **47**, 869 (1993).
[10] B. Dammann and J. D. Reger, Europhys. Lett. **21**, 157 (1993); Z. Phys. B **98**, 97 (1995).
[11] J. Adler, in *Annual Reviews of Computational Physics IV*, edited by D. Stauffer, p. 241 (World Scientific, Singapore, 1996).
[12] B. I. Halperin, P. C. Hohenberg, and S. Ma, Phys. Rev. Lett. **29**, 1548 (1972).
[13] C. De Dominicis, E. Brézin, and J. Zin-Justin, Phys. Rev. B **12**, 4945 (1975).
[14] R. Bausch, V. Dohm, H. K. Janssen, and R. K. P. Zia, Phys. Rev. Lett **47**, 1837 (1981).
[15] Y. Achiam, J. Phys. A **13**, 1355 (1980).
[16] G. F. Mazenko and O. T. Valls, Phys. Rev. B **24**, 1419 (1981); *ibid.* **31**, 1565 (1985).
[17] H. Takano and M. Suzuki, Prog. Theor. Phys. **67**, 1332 (1982).
[18] F. Haake, M. Lewenstein, and M. Wilkens, Z. Phys. B **54**, 333 (1984).
[19] J. Tobochnik, S. Sarker, and R. Cordery, Phys. Rev. Lett. **46**, 1417 (1981).
[20] C. Kalle, J. Phys. A **17**, L801 (1984).
[21] J. K. Williams, J. Phys. A **18**, 49 (1985).
[22] M.-D. Lacasse, J. Viñals, and M. Grant, Phys. Rev. B **47**, 5646 (1993).
[23] S.-K. Ma, Phys. Rev. Lett. **37**, 461 (1976); R. H. Swendsen, Phys. Rev. Lett. **42**, 859 (1979); R. H. Swendsen, in *Real Space Renormalization*, edited by T. W. Burkhardt and J. M. J. van Leeuwen (Springer, Berlin, 1982).
[24] E. Stoll, K. Binder, and T. Schneider, Phys. Rev. B **8**, 3266 (1973).
[25] S. Tang and D. P. Landau, Phys. Rev. B **36**, 567 (1987); S. Wansleben and D. P. Landau, Phys. Rev. B **43**, 6006 (1991).
[26] D. P. Landau, Physica A **205**, 41 (1994).
[27] R. B. Pearson, J. L. Richardson, and D. Toussaint, Phys. Rev. B **31**, 4472 (1985).
[28] H.-O. Heuer, J. Phys. A **25**, L567 (1992); in *Annual Reviews of Computational Physics IV*, edited by D. Stauffer, p. 267 (World Scientific, Singapore, 1996).
[29] M. Kikuchi and Y. Okabe, J. Phys. Soc. Jpn, **55**, 1359 (1986).
[30] O. F. de Alcantara Bonfim, Europhys. Lett. **4**, 373 (1987).
[31] M. Mori and Y. Tsuda, Phys. Rev. B **37**, 5444 (1988).
[32] D. Stauffer, Physica A **184**, 201 (1992); *ibid.* **186**, 197 (1992); Int. J. Mod. Phys. C **3**, 1059 (1992); G. A. Kohring and D. Stauffer, Int. J. Mod. Phys. C **3**, 1165 (1992).
[33] C. Münkel, D. W. Heermann, J. Adler, M. Gofman, and D. Stauffer, Physica A **193**, 540 (1993); C. Münkel, Int. J. Mod. Phys. C **4**, 1137 (1993); A. Linke, D. W. Heermann, P. Altevogt, and M. Siegert, Physica A **222**, 205 (1995).
[34] N. Ito, Physica A **196**, 591 (1993); *ibid.* **192**, 604 (1993).
[35] D. Stauffer, Phys. A **26**, L599 (1993).
[36] R. Matz, D. L. Hunter, and N. Jan, J. Stat. Phys. **74**, 903 (1994).
[37] P. Grassberger, Physica A **214**, 547 (1995).
[38] U. Gropengiesser, Physica A **215**, 308 (1995).
[39] F. Wang, N. Hatano, and M. Suzuki, J. Phys. A **28** 4543 (1995). F. Wang and M. Suzuki, Physica A **220**, 534 (1995). F.-G. Wang and C.-K. Hu, Phys. Rev. E **56**, 2310 (1997).
[40] M. Kikuchi, N. Ito, and Y. Okabe, in *Computer Simulation Studies in Condensed-Matter Physics VII*, edited by D. P. Landau, K. K. Mon, and H. B. Schüttler, p. 44 (Springer, Berlin, 1994).
[41] Z. B. Li, L. Schülke, and B. Zheng, Phys. Rev. Lett. **74**, 3396 (1995).
[42] M. S. Soares, J. K. L. da Silva, and F. C. Sá Barreto, Phys. Rev. B **55**, 1021 (1997).
[43] R. Pandit, G. Forgacs, and P. Rujan, Phys. Rev. B **24**, 1576 (1981).
[44] M. P. Nightingale and H. W. J. Blöte, Phys. Rev. Lett. **76**, 4548 (1996).
[45] R. J. Glauber, J. Math. Phys. **4**, 294 (1963).
[46] L. Onsager, Phys. Rev. **65**, 117 (1944).
[47] H. Müller-Krumbhaar and K. Binder, J. Stat. Phys. **8**, 1 (1973).
[48] R. H. Swendsen and J.-S. Wang, Phys. Rev. Lett. **58**, 86 (1987); J.-S. Wang and R. H. Swendsen, Physica A **167**, 565 (1990).
[49] C. K. Gan and J.-S. Wang, J. Phys. A **29**, L177 (1996); Phys. Rev. E **55**, 107 (1997); J. Chem. Phys. (to appear).
[50] V. Privman, ed., *Finite Size Scaling and the Numerical Simulation of Statistical Systems* (Singapore, Word Scientific, 1990).
[51] M. Suzuki, Prog. Theor. Phys. **58**, 1142 (1977).
[52] E. Domany, Phys. Rev. Lett. **52**, 871 (1984).
[53] G. A. Baker and P. Graves-Morris, *Padé Approximants, Encyclopedia of Mathematics and its Applications*, Vol. 13, and Vol. 14 (Reading, Mass. Addison-Wesley, 1981).
[54] A. J. Guttmann, in *Phase Transitions and Critical Phenomena*, Vol. 13, edited by C. Domb and J. L. Lebowitz (Academic, New York, 1989).
[55] R. Dickman, J.-S. Wang, I. Jensen, J. Chem. Phys. **94**, 8252 (1991); I. Jensen and R. Dickman, J. Stat. Phys. **71**, 89 (1993).
[56] D. Stauffer, Physica A **215**, 305 (1995).

TABLE I. CPU time and memory usage for the series expansion of relaxation of magnetization, measured on an AlphaStation 250/266.

n	CPU time (sec)	Memory (MB)
6	0.13	0.03
7	1.8	0.27
8	25	3
9	358	34
10	23600	51
11	939000	70
12[a]	1.6×10^7	85

[a]Actual computations are done on a 16-node Pentium Pro 200 cluster.

TABLE II. Series-expansion coefficients (n-th derivative) for a single spin $\langle\sigma_0\rangle_t$ and nearest neighbor spin correlation $\langle\sigma_0\sigma_1\rangle_t$.

n	$\frac{d^n\langle\sigma_0\rangle_t}{dt^n}\vert_0$	$\frac{d^n\langle\sigma_0\sigma_1\rangle_t}{dt^n}\vert_0$
0	1	1
1	$-1+(2\sqrt{2})/3$	$-2+(4\sqrt{2})/3$
2	$13/9-\sqrt{2}$	$(56-39\sqrt{2})/9$
3	$(15-11\sqrt{2})/27$	$2(-249+175\sqrt{2})/27$
4	$-53/3+25/\sqrt{2}$	$(1988-1399\sqrt{2})/54$
5	$(41175-29111\sqrt{2})/486$	$(30834-21919\sqrt{2})/486$
6	$(-66133+46680\sqrt{2})/1458$	$2(-142869+101087\sqrt{2})/243$
7	$(-125718825+88903747\sqrt{2})/34992$	$5(18191091-12867401\sqrt{2})/17496$
8	$17(92513582-65418301\sqrt{2})/34992$	$(2190719830-1548846809\sqrt{2})/69984$
9	$(-429437553903+303660675715\sqrt{2})/1259712$	$(-289028693217+204371192813\sqrt{2})/314928$
10	$(4931635327666-3487215692619\sqrt{2})/3779136$	$(43146864055759-30509318092215\sqrt{2})/3779136$
11	$(1821425391381531-1287938652305897\sqrt{2})/181398528$	$(-957792089655213+677259915390707\sqrt{2})/10077696$
12	7(–1076163667757321+$760962133026802 5\sqrt{2}$)$/272097792$	$(425962164223774298$–$301200006005168631\sqrt{2})/1088391168$

FIG. 1. Padé estimates of the dynamical critical exponent z using $G_1(t=\infty)$, plotted as a function of Δ, the transformation parameter. On this scale, the Padé approximant of order $[N,D]$ is indistinguishable from $[D,N]$.

FIG. 2. Effective exponent $z_{\rm eff}(t)$ plotted against inverse time $1/t$. The circles are Monte Carlo estimates based on Eq. (28); the continuous curve is obtained from the $[6,6]$ Padé approximant of G_1 in variable u, transformed back to F through Eq. (25).

Fig.2, Wang & Gan

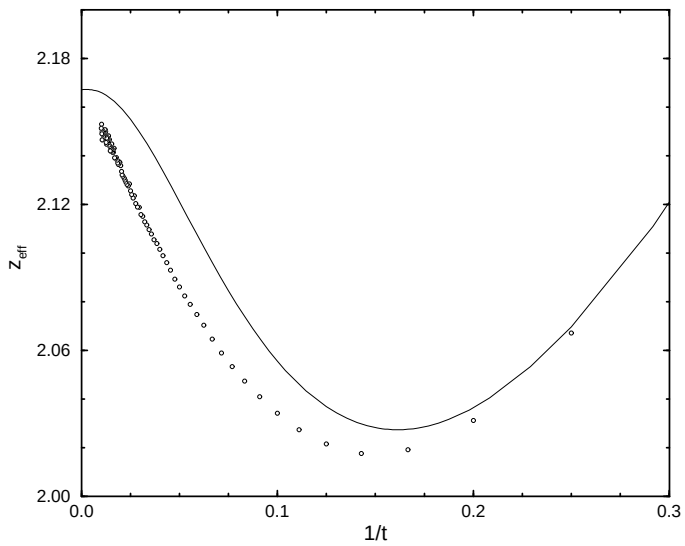

Fig.1, Wang & Gan